

# 1 NetMHCpan 4.0: Improved peptide-MHC class I 2 interaction predictions integrating eluted ligand and 3 peptide binding affinity data<sup>1</sup>

4  
5 Vanessa Jurtz <sup>†</sup>, Sinu Paul <sup>‡</sup>, Massimo Andreatta <sup>§</sup>, Paolo Marcatili <sup>†</sup>, Bjoern Peters <sup>‡</sup>, and Morten  
6 Nielsen <sup>†,§,\*</sup>

7  
8 <sup>†</sup> Department of Bio and Health Informatics, Technical University of Denmark, DK-2800  
9 Lyngby, Denmark

10 <sup>‡</sup> Division of Vaccine Discovery, La Jolla Institute for Allergy and Immunology, CA92037 La  
11 Jolla, USA

12 <sup>§</sup> Instituto de Investigaciones Biotecnológicas, Universidad Nacional de San Martín, CP1650 San  
13 Martín, Argentina

14  
15 \* Corresponding author [mniel@cbs.dtu.dk](mailto:mniel@cbs.dtu.dk)

16  
17 Running title: Improved peptide-MHC class I interaction predictions

## 18 Abstract

19 Cytotoxic T cells are of central importance in the immune system's response to disease. They  
20 recognize defective cells by binding to peptides presented on the cell surface by MHC (major  
21 histocompatibility complex) class I molecules. Peptide binding to MHC molecules is the single  
22 most selective step in the antigen presentation pathway. On the quest for T cell epitopes, the  
23 prediction of peptide binding to MHC molecules has therefore attracted large attention.  
24 In the past, predictors of peptide-MHC interaction have in most cases been trained on binding  
25 affinity data. Recently an increasing amount of MHC presented peptides identified by mass  
26 spectrometry has been published containing information about peptide processing steps in the  
27 presentation pathway and the length distribution of naturally presented peptides. Here, we  
28 present NetMHCpan-4.0, a method trained on both binding affinity and eluted ligand data  
29 leveraging the information from both data types. Large-scale benchmarking of the method  
30 demonstrates an increased predictive performance compared to state-of-the-art when it comes to  
31 identification of naturally processed ligands, cancer neoantigens, and T cell epitopes.

---

<sup>1</sup> This work was supported by Federal funds from the National Institute of Allergy and Infectious Diseases, National Institutes of Health, Department of Health and Human Services, under Contract No. HHSN272201200010C and from the Agencia Nacional de Promoción Científica y Tecnológica, Argentina (PICT-2012-0115).

32

## 33 Introduction

34 Cytotoxic T cells play a central role in the immune regulation of pathogenesis and malignancy.  
35 They perform the task of scrutinizing the surface of cells for the non-self peptides presented in  
36 complex with MHC (major histocompatibility complex) molecules. In cases such peptides are  
37 recognized, an immune response can be initiated potentially leading to killing of the infected  
38 (mal-functioning) cell. The most selective step in the pathway leading to this peptide  
39 presentation is the binding to MHC.

40  
41 Over the last decades, large efforts have been dedicated to the development of computational  
42 methods capable of accurately predicting this event. The accuracy of these methods has  
43 improved substantially over the last years, and most recent benchmark results demonstrate that  
44 more than 90% of naturally presented MHC ligands are identified at an impressive specificity of  
45 98% (1). This gain in performance is achieved partly by the extended experimental binding data  
46 sets made available in the IEDB (2), and partly by the development of novel machine-learning  
47 algorithms capable of capturing the information in the experimental binding data in a more  
48 effective manner. One such novel method is NNAlign-2.0, allowing the integration of peptides of  
49 variable length into the machine-learning framework (3). This novel training approach allows  
50 both the incorporation of a larger set of training data, but also and maybe more importantly  
51 enables the method to directly learn the length preference presented peptides for each MHC  
52 molecule from the experimental binding data (4). Even though most presented MHC class I  
53 ligands are of length 9 amino acids, the ability to incorporate length preferences directly into the  
54 model is critical as experimental data demonstrate that the length profiles of presented ligands  
55 can vary substantially between MHC molecules; prominent examples are the mouse H-2-Kb,  
56 with a preference for eight amino acids-long peptides (5) and HLA-A\*01:01, where close to one  
57 third of MHC presented peptides have a length longer than nine amino acids (6).

58  
59 Some of the most well documented and applied of methods for predicting peptide binding to  
60 MHC class I include NetMHC (4,7), and NetMHCpan (1,8). These tools have over the last years  
61 gained increasing interest due to the recent focus on neoantigen identification within the field of  
62 personalized immunotherapy (9,10). However, as underlined in several studies including the  
63 recent Nature Biotechnology Editorial (11), “neoantigen discovery and validation remains a  
64 daunting problem”, mostly due to the relative high false positive rate of predicted epitopes.

65  
66 One potential cause for this relatively high rate of false positive epitope predictions is the fact  
67 that most methods are trained on binding affinity data, and as a consequence only model the  
68 single event of peptide-MHC binding. As stated above this binding to MHC is the most selective  
69 step in peptide antigen presentation. However, other factors including antigen processing (12)  
70 and the stability of the peptide:MHC complex (13) could influence the likelihood of a given  
71 peptide to be presented as an MHC ligand. Similarly, the length distribution of peptides available  
72 for binding to MHC molecules is impacted by other steps in the processing and presentation  
73 pathway, such as TAP transport and ERAP trimming, which are not reflected in binding data in  
74 itself (6). Advances in mass spectrometry (MS) have allowed the field of MS peptidomics to  
75 move forward. In this context, recent studies (14,15,16) have suggested that training prediction

76 methods on such data rather than binding affinity data could improve the ability to accurately  
77 identify MHC ligands. As such, MS peptidome data would contain the comprehensive signal of  
78 antigen processing and presentation rather than just MHC binding affinity. Moreover, MS  
79 peptidome data generated by immunopeptidomic studies would contain precise information  
80 about the allele-specific peptide length profile preferences not available in the MHC binding  
81 affinity data sets.

82  
83 Identification of MHC bound peptides by mass spectrometry thus holds great promise for the  
84 generation of large scale data sets characterizing the peptidome specific for individual MHC  
85 molecules (15,17), and potentially also for the identification of T cell epitopes (18). It is  
86 however clear that, within the foreseeable future, the number of MHC molecules characterized  
87 by such MS studies will remain limited. In this context, large efforts have over the last decades  
88 been dedicated to experimentally characterize the peptide binding space of MHC molecules  
89 using semi high-throughput MHC-peptide binding affinity assays (19,20), enabling binding  
90 specificity characterization of a large set of MHC molecules from different species.

91  
92 The IEDB contains a comprehensive set of MHC binding and ligand data available in the public  
93 domain. While this data set contains binding affinity data characterizing more than 150 different  
94 MHC class I molecules (from human, non-human primates, mouse, and life-stock), at the onset  
95 of this study only 55 MHC class I molecules were characterized by MS peptidome data. This  
96 imbalance made us suggest a novel machine learning approach integrating information from both  
97 types of data (binding affinity and MS ligands) into a combined framework benefitting from  
98 information from the two worlds. The proposed framework is “pan-specific” as it can leverage  
99 information across MHC molecules, data types, and peptide lengths into one single model. We  
100 hence expect this approach to achieve superior predictive performance compared to models  
101 trained on the two data types individually, and also achieve an improved performance when it  
102 comes to predicting length profile preferences of different MHC molecules.

103  
104 While recent works have demonstrated the improved ability to identify MHC ligands using  
105 methods trained on MS peptidome data (14,15), limited data is available on their impact for the  
106 identification of T cell epitopes. In this work, we focus on demonstrating the improved  
107 prediction performance not only on large sets of MS peptidome data but also on T cell epitope  
108 data independent from the data used to train the new predictor.  
109

## 110 **Materials and Methods**

### 111 **Data sets**

112  
113 Data on all class I MHC ligand elution assays available in IEDB database ([www.iedb.org](http://www.iedb.org)) were  
114 collected including the ligand sequence, details of the source protein, position of the ligand in the  
115 source protein and the restricting allele of the ligand. There were 160,527 distinct assays in total  
116 and the length of the ligands ranged from 4-37. All lengths with a count of ligands at least 0.5%  
117 of total ligands were selected for further analysis which included lengths 8-15 and comprised of  
118 99% of the assay entries.

119  
120 The restricting MHC molecule of the ligands were analyzed and entries with alleles listed  
121 unambiguously were selected. For example, some entries where the HLA alleles are listed as just  
122 the gene name and alleles from chicken, horse, cow and mouse for which we did not have  
123 binding prediction algorithms were excluded. Representative alleles were assigned for entries  
124 where only supertypes were listed (e.g. HLA-A\*26:01 for HLA-A26). Thus there were 127 class  
125 I molecules from human and mouse in the selected data set. Redundant entries with same ligand  
126 sequence and MHC molecule were removed and MHC molecules with at least 50 ligand entries  
127 were selected. This included 55 class I molecules and the number of available ligands per  
128 molecule varied widely from 50 to 9500.

129  
130 We hypothesized that some of the ligands could be artefacts of the elution assays and therefore  
131 their source proteins could be false positive as antigens. A protocol was designed to identify such  
132 false positive antigens and exclude them from the final data selected. The protocol identified  
133 proteins that had significantly lesser number of predicted binders among ligands than expected of  
134 random peptides using binomial probability distribution. Five sets of random peptides were  
135 generated from the ligand sequences by shuffling the amino acid residues within the ligands.  
136 Binding affinity was then predicted for the original ligands and random peptide sets for their  
137 corresponding alleles. The median of the predicted percentile ranks of the five random sets was  
138 estimated and assigned as the binding affinity of the random peptides. Based on a predicted  
139 binding affinity cut-off of percentile rank 1.0, the number of predicted binders among the  
140 original ligands and the random peptide sets were estimated. Five proteins were thus identified as  
141 false positives and ligand entries from these proteins were excluded from the data set.

142  
143 The final data set had 85,217 entries in total with ligand length ranging from 8 to 15. The ligands  
144 originated from 14,797 source antigens and were restricted by 55 unique HLA molecules.

145  
146 Random artificial negatives were generated for each MHC molecule covered by eluted ligand  
147 data by sampling randomly  $10 \times N$  peptides of each length 8-15 amino acids from the antigen  
148 source protein sequences, where N is the number of 9mer ligands for the given MHC molecule.

## 149 Neural network training

150 The NNAlign training approach with insertions and deletions (3) was extended by adding a  
151 second output neuron as shown in figure 1. This was done to allow combined training on binding  
152 affinity and MS eluted ligand data. Binding affinity values are measured as IC50 values in nM  
153 (aff) and can be rescaled to the interval [0,1] by applying  $1 - \log(\text{aff}) / \log(50,000)$ , representing  
154 continuous target values (21). For eluted ligands the strength of the interaction between peptide  
155 and MHC molecules is unknown, therefore a target value of 1 is assigned to binders and 0 to  
156 artificial negative peptides (see above).

157  
158 In this network architecture weights between the input and hidden layer are shared between the  
159 two input types (binding affinity/ligand), and weights connecting the hidden and output layer are  
160 specific for each input type. During neural network an example is randomly selected from either  
161 data set and submitted to forward- and backpropagation according to the NNAlign algorithm (3).  
162 In this setting, we define one training epoch as the average number of iterations needed to  
163 process each data point in the smaller data once.

164  
165 A neural network ensemble was trained as described by Andreatta et al. (1) using 5-fold nested  
166 cross-validation. Networks with 60 and 70 hidden neurons were trained leading to an ensemble  
167 of 40 networks in total.

168  
169 The inputs to the neural networks consisted of the peptide and the MHC molecule in terms of a  
170 pseudo sequence (8). All peptides were represented as 9-mer binding cores by the use of  
171 insertions and deletions as described by Andreatta et al. (4) and encoded using BLOSUM  
172 encoding (21). As in the earlier work by Andreatta et al. (4), additional features for the encoding  
173 of peptides included: the length of the deletion/insertion; the length of peptide flanking regions,  
174 which are larger than zero in the case of a predicted extension of the peptide outside either  
175 terminus of the binding groove; and the length L of the peptide, encoded with four input neurons  
176 corresponding to the four cases  $L \leq 8$ ,  $L=9$ ,  $L=10$ ,  $L \geq 11$ .

## 177 Performance

178 In order to benchmark the combined training method described above (referred to as BA+EL),  
179 additional methods with only one output but otherwise identical setup were trained on binding  
180 affinity data only (BA data) and eluted ligand data only (EL method). Performance was  
181 measured as area under the receiver operating curve (AUC), a value of  $AUC=0.5$  indicates  
182 random model performance while an  $AUC=1$  represents a perfect model. AUC values were  
183 calculated for each MHC allele separately and subsequently binomial tests were performed to  
184 compare the different models.

## 185 Length preference of MHC molecules

186 For all MHC molecules shared between the binding affinity and eluted ligand data sets, we  
187 generated predictions for 80,000 random natural peptides of lengths 8-15 amino acids (10,000 of  
188 each length). From the top 2% predictions, the frequency of each peptide length was estimated.  
189 Subsequently Pearson's correlation coefficient was calculated between the frequencies observed  
190 in the eluted ligand data set and the frequencies predicted by 4 models (BA only, EL only,  
191 binding affinity of BA+EL, and eluted ligand predictions of BA+EL)

## 192 Leave-one-out validation

193 Leave-one-out experiments were performed for all MHC molecules present in the eluted ligand  
194 data set. For this, a given MHC molecule was removed from the eluted ligand data set, then the  
195 BA+EL method was trained in five-fold cross-validation as described above, omitting multiple  
196 random initializations, resulting in an ensemble of 10 networks. Performance of the leave-one-  
197 out models is compared to an ensemble of neural networks of the same size trained on the  
198 complete data set. Further predictions are made for 80,000 peptides of lengths 8-15 amino acids  
199 derived from natural proteins to evaluate a model's ability to predict the length preference of an  
200 MHC allele that was not part of the eluted ligand training data.

## 201 The final NetMHCpan-4.0 method implementation

202 The final neural network ensemble of the NetMHCpan-4.0 method is trained on binding affinity  
203 and eluted ligand data as described above using 5-fold cross-validation. Networks with 56 and 66  
204 hidden neurons (in accordance with earlier NetMHCpan implementations) were trained using 10  
205 distinct random initial configurations, leading to an ensemble of 100 networks in total.

206  
207 Percentile rank scores was estimated from predicted EL and BA binding values from a set of  
208 125,000 8-12mer random natural peptides (25,000 of each length)

## 209 Validation on external data sets

210  
211 A dataset of eluted ligands was obtained from Pearson et al. (17). Also, a set of positive CD8  
212 epitopes was downloaded from the IEDB. The epitope set was identified using the following  
213 search criteria "T cell assays: IFNg", "positive assays only", "MHC restriction Type: Class I".  
214 Only entries with fully typed HLA restriction, peptides length in the range 8-14 amino acids, and  
215 with annotated source protein sequence were included. Positive entries with a predicted rank  
216 score greater than 10% using NetMHCpan-3.0 were excluded to filter out likely noise (6). For  
217 both the T-cell epitope and eluted ligand data sets, negative peptides were obtained by extracting  
218 all 8-14mer peptides from the source proteins of the eluted ligands and subsequently excluding  
219 peptides-MHC combination found with an exact match in the training data (both binding affinity  
220 and eluted ligand data sets). The final eluted data set contained 15,965 positive ligands restricted  
221 to 27 different HLA molecules, and the IEDB T cell epitope data set 1,251 positive T cell  
222 epitopes restricted to 80 HLA molecules.

223  
224 A Frank value was calculated for each positive-HLA pair as the ratio between the number of  
225 peptides with a prediction score higher than the positive peptide and the number of peptides  
226 contained within the source protein. The Frank value is hence 0 if the positive peptide has the  
227 highest prediction value of all peptides within the source protein, and a value of 0.5 in cases  
228 where an equal amount of peptides has a higher and lower prediction value compared to the  
229 positive peptide.

230  
231 An unfiltered eluted ligand data set was obtained from Bassani-Sternberg et al. (22). This data  
232 sets consisted of eluted ligand data from 6 cell lines each with fully typed HLA-A, B and C  
233 alleles. A data set was constructed for each cell line, including all 8-13mer ligand as positives,  
234 and 5 times the total number of ligands random natural negatives for each length 8-13. That is if  
235 a data set contained 5,000 ligands,  $5 \times 5000 = 25,000$  random natural peptides of length 8, 9, 10,  
236 11, 12, and 13 were added as negatives arriving at a final data set with 155,000 ( $5000 +$   
237  $6 \times 25000$ ) peptides.

238

## 239 Results

240 We trained the NetMHCpan method version 4.0 for the prediction of the interaction of peptides  
241 with MHC class I molecules integrating binding affinity and MS eluted ligand data. Combined  
242 training was achieved by adding a second output neuron to the NNAlign approach described

243 previously (3). In this setup, the first output neuron returns a score of binding affinity, and the  
244 second output neuron a score of ligand elution. As described in materials and methods, the model  
245 parameters between the input and hidden layer of the artificial neural network are shared  
246 between the two input types. Thanks to this network architecture, we expect the model to be able  
247 to combine informative patterns found in the two data types, boosting performance for both  
248 output neurons. To demonstrate this, we compared the performance of the BA+EL method to the  
249 BA method, trained only on binding affinity data and the EL method trained only on eluted  
250 ligand data. Figure 2 shows the mean performance per MHC allele of the four methods on four  
251 different data sets given in in terms of AUC (for details see Supplementary Table 1). From this  
252 analysis, it is clear that especially the BA+EL method with EL predictions performs much better  
253 on binding affinity data than the EL only method. This observation strongly suggests that the EL  
254 only method, as a results of the small number of only 55 different MHC molecules included in  
255 the eluted ligand data set, has limited pan-specific potential compared to the BA+EL EL method  
256 trained on data from 169 MHC molecules included in the combined binding and MS eluted  
257 ligand data set.

## 258 Peptide length preference of MHC molecules

259 We next set out to investigate how well the different methods could capture the peptide length  
260 preferences of individual MHC molecules. For this, we predicted binding scores for a set of  
261 random natural peptides of lengths 8-15 amino acids and calculated the frequencies of peptides  
262 of different lengths in the top 2% of predictions. In figure 3a-c, we visualize examples of such  
263 peptide length preference profiles predicted by the BA, BA+EL BA, BA+EL EL, and EL only  
264 methods. The depicted MHC molecules are known to have preferences for different peptide  
265 lengths. All HLAs have a preference for 9mer peptides. However, HLA-A\*01:01 has an  
266 increased preference for 10-mers compared to average, HLA-A\*02:01 has a strong preference  
267 for 9-mers only, and HLA-B\*51:01 has an increased preference for 8-mers compared to average  
268 (6). Binding affinity predictors often overestimate the amount of binding 10-mer peptides due to  
269 their over-representation in the binding affinity data set (4), which is also visualized in figure 3.

270  
271 Next, we extended the analysis to all MHC molecules included in the eluted ligand data set,  
272 calculating the correlation between observed and predicted length frequencies for each prediction  
273 method. This analysis (figure 3d) clearly confirms the results obtained from the 3 case examples,  
274 namely that the two methods BA+EL EL and EL only show significantly higher power for  
275 predicting the peptide length preference of individual MHC molecules compared to the two  
276 methods trained to predict binding affinity (BA, and BA+EL BA).

277  
278 The predictions for the two eluted ligand likelihood models only show low performance for one  
279 molecule; HLA-B41:04. This molecule is however only characterized by 52 eluted ligands,  
280 whose length profile forms an unusual bimodal distribution with peaks at length 9 and 11 (data  
281 not shown).

## 282 Leave-one-out experiments on eluted ligand data

283 In the above experiment, the MHC molecules used for the peptide length preference evaluation  
284 were also included as training data of the EL prediction methods. This naturally leads to a bias  
285 in the performance evaluation. To address this, and to access the pan-specific potential of the

286 BA+EL EL prediction method, we conducted a leave-one-out experiment. Here, a given MHC  
287 molecule was removed from the eluted ligand data set, and the BA+EL method retrained as  
288 described in material and methods. Next, both the predictive performance (estimated in terms of  
289 AUC for separating the known ligands from the artificial negatives) and the ability to predict the  
290 peptide length preference were evaluated. The result of the benchmark is shown in figure 4.  
291 This figure clearly confirms the pan-specific power of the BA+EL method. In terms of the  
292 predictive performance (figure 4a), the LOO methods display, as expected, a slight decrease in  
293 performance compared to a method trained and evaluated on all data (the all data method).  
294 When looking at the performance for predicting the peptide length profile (figure 4b), the LOO  
295 methods display a very high performance. Only in one case, the EL LOO method shows a  
296 substantial drop in performance for the left out MHC molecule. This case is H2-Kb, the only  
297 mouse molecule in the MS ligand data set with a strong preference for 8mer ligands. The  
298 BA+EL EL LOO method is able to predict the length profile of H2-Kb due to the H2-Kb affinity  
299 data present in the BA training data set.

### 300 The NetMHCpan-4.0 method

301 Having demonstrated the increased predictive power of the BA+EL method when it comes to  
302 prediction of peptide binding affinity (the BA+EL BA model), likelihood of being an eluted ligand  
303 (BA+EL EL model), and the ability of capturing the MHC specific peptide length binding  
304 preferences (also the BA+EL EL model), we set out to construct the final NetMHCpan-4.0  
305 method. This method was trained as the BA+EL method, using 5 fold cross-validation as  
306 described in materials and methods. The method is accessible at  
307 [www.cbs.dtu.dk/services/NetMHCpan-4.0](http://www.cbs.dtu.dk/services/NetMHCpan-4.0). The functionality is identical to the earlier  
308 NetMHCpan implementations with the important additional functionality that two different output  
309 options (binding affinity and eluted ligand likelihood) are available. By default, the program  
310 returns eluted ligand likelihood scores. An example of the output of the method is shown in  
311 Supplementary figure 1.

### 312 Validation on external data sets

313 The performance of the updated NetMHCpan method was assessed on two independent external  
314 data sets; one consisting of 15,965 eluted ligands covering 27 HLA molecules, and another  
315 consisting of 1,251 validated CTL epitopes covering 80 HLA molecules reported in the IEDB.  
316 The validation data sets were constructed as described in materials and methods. The source  
317 protein sequence was identified for each ligand/epitope, and all overlapping 8-14 mer peptides  
318 except the ligand/epitope were annotated as negatives. All data points included in the binding  
319 affinity and eluted ligand training data sets were excluded from the validation data set. A Frank  
320 value was calculated for each positive-HLA pair as described in materials and methods as the  
321 ratio of the number of peptides with a prediction score higher than the positive peptide to the  
322 number of peptides contained within the source protein. In this manner, we can construct the  
323 sensitivity curves presented in figure 5. Two observations are striking from these results. First  
324 and foremost, the results clearly demonstrated the increased predictive power of integrating  
325 eluted ligand data into the training data of NetMHCpan. In the left panel (the analysis of the  
326 eluted ligand data), we can observe that the gain in sensitivity at a Frank threshold of 1% for the



327 EL models (NetMHCpan-4.0 EL or EL only) compared to NetMHCpan-3.0 is 10% (95% versus  
328 85%), and 15% at a Frank threshold of 0.5% (90% versus 75%). These numbers mean that a  
329 ligand will have a prediction score within the top 0.5% of its source protein peptides in 90% of  
330 the cases using the EL models, compared to only 75% using NetMHCpan-3.0. The results shown  
331 in the left panel of figure 5 however also suggest that the two EL models achieve very similar  
332 predictive performance when it come to identification of eluted ligands. This is in strong contrast  
333 to the results obtained from the IEDB epitope data set (figure 5, right panel). Here, only the  
334 NetMHCpan-4.0 EL model demonstrates an improved predictive performance compared to  
335 NetMHCpan-3.0.

336  
337 There are several potential explanations for the improved performance of the EL models on the  
338 eluted ligand evaluation data including i) a bias against cysteins specific for the eluted ligand  
339 training and evaluation data, ii) as suggested earlier (15) differences in the MHC binding motifs  
340 contained within the eluted ligand and *in-vitro* binding data, and iii) the improved prediction  
341 accuracy of the ligand length preference (see figure 3d). To investigate i) we repeated the  
342 experiment displayed in figure 5, removing all peptides containing one of more cysteins. If the  
343 bias against cysteins in the eluted ligand data had any impact on the predictive performance of  
344 the proposed method, the bias would be reflected in an altered predictive performance on the  
345 reduced data sets. This turned out not to be the case (data not shown) hence suggesting that  
346 cysteine bias is not the influencing the relative predictive performance of the different methods.  
347 Looking into the differences in the binding motif derived from binding affinity and eluted ligand  
348 data respectively for specific HLA molecules, we find differences for most MHC molecules. A  
349 few examples are shown in figure 6.

350  
351 These results demonstrated that eluted ligands tend to share more conserved anchor motifs  
352 compared to affinity-defined binders. This observation is in agreement with earlier findings  
353 suggesting eluted ligands to be more stably bound to MHC-I molecules compared with other  
354 affinity matched peptides (13,23). In summary, these analyses suggest that the gained predictive  
355 performance of the EL method on the eluted ligand evaluation data is driven by at least two  
356 factors; differences in binding preferences between eluted ligand and affinity-defined peptide  
357 binders, and the improved prediction accuracy of ligand length preference of the EL methods.

## 358 To be or not to be a ligand

359 We investigated what prediction threshold to use to best separate ligand from non-ligand  
360 peptides. Earlier work by others and us suggests that different MHC molecules present peptides  
361 at different predicted binding affinity thresholds (1,24). Given this, it was interesting to  
362 investigate to what degree a similar observation could be made for the eluted ligand likelihood  
363 predictions produced by the NetMHCpan-4.0 method. To address the question, we compared the  
364 predicted ligand likelihood scores of all 15,965 ligands in the Pearson data set. The result of this  
365 analysis is displayed as box-plots in the left panel of figure 7.

366  
367 This figure reveals that the likelihood prediction scores for known ligands come out very  
368 different for different HLA molecules. The large difference in prediction values between HLA  
369 molecules can to a high degree be linked to their absence from the eluted ligand training data.  
370 The molecules with lowest median eluted ligand likelihood scores in this figure are molecules  
371 absent from the eluted ligand training data set. However, as demonstrated in figure 4 and 5, the

372 fact that an HLA molecule has not been characterized with eluted ligand training data does not  
373 impair its predictability. Given this, a natural measure to correct for this great imbalance in  
374 prediction score is use percentile rank scores to reconcile and make prediction score comparable  
375 between different MHC molecules. The right panel of figure 7 shows the results of such a  
376 transformation. Here, eluted ligand likelihood prediction values for each ligand in the Pearson  
377 data are transformed to percentile rank scores, and the score distribution is visualized as box  
378 plots for each HLA molecule. Given that percentile rank values fall in the range 0-100%, it is  
379 apparent that transforming the prediction values into such rank scores, allows for a direct score  
380 comparison between HLA molecules.

381  
382 In light of these results, we next investigated what percentile rank threshold to apply to optimally  
383 identify MHC ligands. We assess this by calculating sensitivity/specificity curves as a function  
384 of the percentile rank score threshold for a balanced set (max 100 ligands per HLA) of eluted  
385 ligands and source protein negatives from the Pearson evaluation data set. The results are shown  
386 in figure 8 and confirm earlier findings that the vast majority (96.5%) of natural ligands are  
387 identified at a very high specificity (98.5) using a percentile rank threshold of 2%.

## 388 Evaluation on unbiased data sets

389 Most eluted ligand data potentially suffer from biases towards current prediction methods. This  
390 is because many eluted ligand studies, including the Pearson data used here, assign MHC  
391 restriction based on predicted binding. To address the impact of this bias, we here benchmark our  
392 method against sets of unfiltered eluted ligand data. These data sets were obtained from Bassani-  
393 Sternberg et al. (22), and cover eluted ligands obtained from 6 cell lines each with typed HLA  
394 expression. From these data, we constructed 6 benchmark data sets by enriching each positive  
395 eluted ligand data set with a set of random natural negative peptides (for details see materials and  
396 methods). After filtering out data included in the training data of NetMHCpan-4.0, we next  
397 benchmarked the predictive power of the different prediction methods. The result of the  
398 benchmark is shown in figure 9.

399  
400  
401 These results clearly confirm the improved performance of the proposed NetMHCpan-4.0 eluted  
402 ligand likelihood predictions over both the NetMHCpan-4.0 and NetMHCpan-3.0 binding  
403 affinity predictions. Also, the results show that in the majority of cases the percentile rank  
404 predictions achieve improved predictive performance compared to the raw prediction scores.

## 405 Identification of cancer neoantigens

406 A research field where prediction of naturally processed and presented eluted ligand has attracted  
407 large recent attention is rational identification of cancer neoantigens. In contrast to tumor-  
408 associated self-antigens, cancer neoantigen are naturally presented ligands containing tumour-  
409 specific mutations. Such neoantigens are attracting large attention since these peptides are new to  
410 the immune system and not found in normal tissues, and hence are ideal potential cancer vaccine  
411 candidates or targets for adoptive T cell therapy. Depending on the mutational load, the number  
412 of potential tumour-specific neopeptides (peptides containing one or more missense mutations)  
413 can be in the order of many thousands (25). This large number of potential peptide candidates  
414 clearly underlines the need for tools to rationally downsize the peptide space in the search for

415 cancer neoepitopes. A recent study by Bassani-Sternberg et al. (14) demonstrated how this  
416 downsizing could be effectively achieved by a prediction method trained on a large set of MS  
417 eluted ligands. Here, we repeated this benchmark analysis using NetMHCpan-4.0. The results are  
418 shown in figure 10 and confirm the finding by Bassani-Sternberg et al. (14), that predictors  
419 trained on MS eluted ligand data information in most cases show very high predictive power for  
420 the identification of cancer neoantigens. Both the NetMHCpan-4.0 and MixMHCpred method  
421 proposed by Bassani-Sternberg et al. (14) identify the known neoantigens within the top 25  
422 peptides in 6 out of 10 cases. NetMHCpan-3.0 only achieves this in 2 out of 10 cases. The  
423 results also confirm the earlier findings presented here, that NetMHCpan-4.0 achieves improved  
424 performance compared to that of version 3.0, and that the ligands in all cases are predicted with  
425 very strong eluted ligand likelihood values (all percentile rank values are less than 1, and the  
426 majority are less than or equal to 0.02).

## 427 Discussion

428 In this work, we have demonstrated how a relatively simple pan-specific machine learning  
429 method based on the NNAlign framework can be constructed integrating information from  
430 binding affinity data with MS peptidome data. Benefitting from the larger set of peptide binding  
431 affinity data with very broad MHC coverage (more than 150 molecules), and the additional  
432 information contained within MS peptidome data (information about both antigen processing  
433 and presentation, and allele specific peptide length profile), we could demonstrate that the  
434 proposed method, NetMHCpan-4.0, achieved improved predictive performance not only when it  
435 comes to characterizing the binding specificity of a given MHC molecule, but also when it  
436 comes to predicting the peptide length profile. Due to the pan-specific potential of the method,  
437 the improved performance was extended beyond the relatively few MHC molecules  
438 characterized by MS binding data included in the training of the method. Given this, we thus  
439 conclude that the proposed framework is able to benefit from the best of the two data sets; MHC  
440 coverage from the binding affinity data, and antigen processing and presentation, and allele  
441 specific peptide length profile from the MS data.

442  
443 Our benchmarks confirmed earlier findings that prediction values for known ligands vary  
444 substantially between MHC molecules (26), and that only by the use of percentile rank scores  
445 can predictions between different MHC molecules be readily compared.

446  
447 The improved peptide-MHC tool is made publicly available at  
448 [www.cbs.dtu.dk/services/NetMHCpan-4.0](http://www.cbs.dtu.dk/services/NetMHCpan-4.0). The tool was benchmarked on two large independent  
449 data sets; one consisting of ~16,000 MS identified MHC restricted ligands (17) and one  
450 consisting of more than 1,250 validated T cell epitopes described in the IEDB. For both data sets,  
451 the updated version 4.0 of NetMHCpan significantly outperformed the earlier NetMHCpan 3.0  
452 method. In particular, the benchmark on T cell epitope data - to the best of our knowledge -  
453 demonstrated for the first time how integration of MS peptidome data into a prediction method  
454 of MHC peptide presentation, can lead to improved predictive performance for T cell epitope  
455 discovery. The improved performance on this data set was only observed for the method trained  
456 on the combined data, and was not observed for the method trained on MS peptidome data alone.  
457 This observation underlines the large benefit of merging the two data types.

458

459 Investigating potential causes for the observed improved performance of the proposed tool for  
460 identification of eluted ligands confirmed earlier findings that eluted ligands share a reduced  
461 amino acid diversity at the MHC anchor positions (13). This observation is consistent with the  
462 notion that ligands are more stably bound to MHC-I molecules compared with average affinity-  
463 defined bound peptides. We postulate that this difference in binding preferences between eluted  
464 ligand and affinity-defined peptide binders, combined with the improved prediction accuracy of  
465 ligand length preference of the EL methods are the main factors driving the improved predictive  
466 performance.

467  
468 When benchmarking the predictive performance for identification of T cell epitopes, we  
469 observed that only the NetMHCpan-4.0 EL model trained on the combined eluted ligand and  
470 binding affinity data set demonstrated an improved predictive performance compared to  
471 NetMHCpan-3.0. This observation was surprising at first, as we would expect an improved  
472 performance also by the method trained on the eluted ligand only due to the reasons outlined  
473 above. One likely explanation for this result is the bias in the T cell epitope data towards  
474 predicted binding affinity motifs. Most T cell epitopes have been identified using some kind of  
475 HLA binding predictions as a filter prior to experimental validation hence giving a bias towards  
476 prediction methods trained based on binding affinity data. Given this, the source of the improved  
477 performance of the NetMHCpan-4.0 EL method compared to NetMHCpan-4.0 BA on the T cell  
478 epitope benchmark data set is thus primarily driven by its improved prediction of the ligand  
479 length preference.

480  
481 It is clear that even with the improved predictive performance of the NetMHCpan-4.0 tool  
482 reported here, not all MHC ligands and T cell epitopes will be captured by a prediction  
483 workflow. Likewise, it is clear that very few if any experimental workflows enable the  
484 exhaustive identification of the ligandome or epitope set contained within a given sample. Given  
485 the two workflows to work in concert and use *in-silico* screens as a guide to the experimental  
486 setup to effectively boost the sensitivity of the combined workflow. Such an approach where *in-*  
487 *silico* predictions were used to reduce the search space has with success been used to improve the  
488 sensitivity of MHC class I ligand discovery (27) and we expect other similar applications to  
489 appear in the future.

490  
491 The machine-learning framework proposed here is not limited to the integration of MHC class I  
492 peptide binding affinity and MS peptidome data. The approach can readily be extended to  
493 integrate other types of relevant data including MHC binding stability (28), and epitope data.  
494 Also, the approach can in its current form be directly applied to the MHC class II system. The  
495 only critical limitation for such data integrations is the criteria that each data point must be  
496 associated with a specific MHC element. This information is not always readily available, but  
497 can in most cases be inferred by unsupervised clustering of the available data (using  
498 GibbsCluster (29), position weight matrix mixture models (16), or similar approaches), and  
499 association of each cluster to an MHC molecule of the given host.

500  
501 In conclusion, we have here described a new framework for training of prediction methods for  
502 MHC peptide presentation prediction integrating information from two data sources (MS eluted  
503 ligand and peptide binding affinity). The framework was used to develop an updated version of  
504 NetMHCpan (version 4.0, available at [www.cbs.dtu.dk/services/NetMHCpan-4.0](http://www.cbs.dtu.dk/services/NetMHCpan-4.0)) with

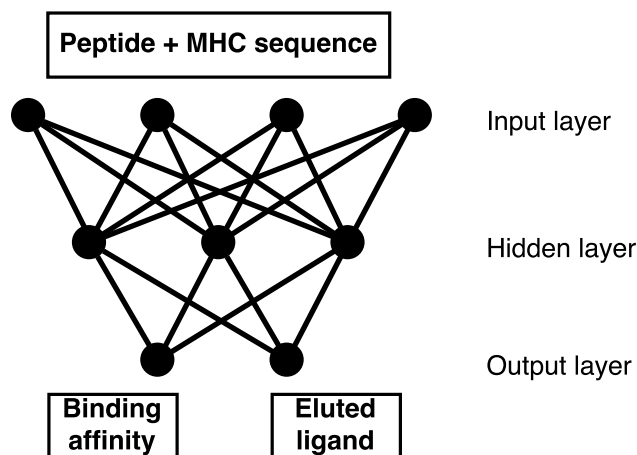
505 improved predictive performance for identification of validated eluted ligands, cancer  
506 neoantigens and T cell epitopes.  
507

## 508 References

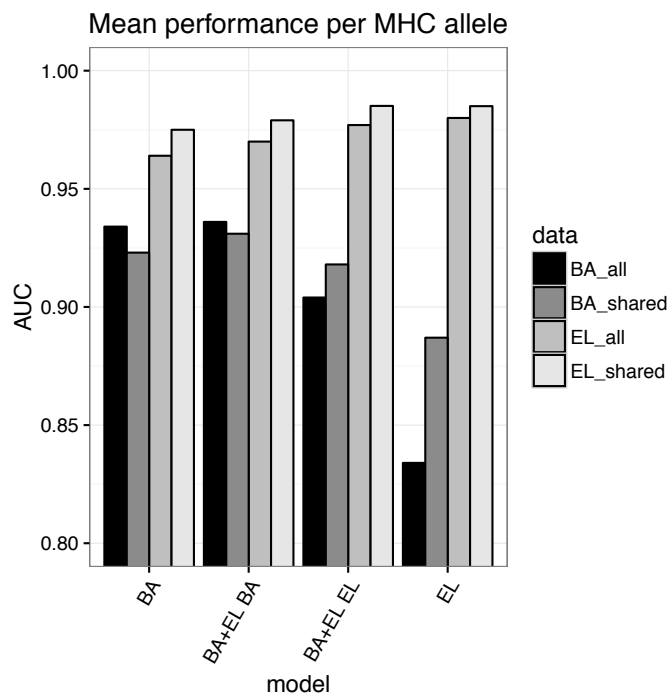
- 509 1. Nielsen, M., and M. Andreatta. 2016. NetMHCpan-3.0; improved prediction of binding to MHC class I  
510 molecules integrating information from multiple receptor and peptide length datasets. *Genome Med.* 8: 1–  
511 9.
- 512 2. Vita, R., J. A. Overton, J. A. Greenbaum, J. Ponomarenko, J. D. Clark, J. R. Cantrell, D. K. Wheeler, J.  
513 L. Gabbard, D. Hix, A. Sette, and B. Peters. 2015. The immune epitope database (IEDB) 3.0. *Nucleic  
514 Acids Res* 43: D405-12.
- 515 3. Nielsen, M., and M. Andreatta. 2017. NNAlign: a platform to construct and evaluate artificial neural  
516 network models of receptor-ligand interactions. *Nucleic Acids Res.* .
- 517 4. Andreatta, M., and M. Nielsen. 2015. Gapped sequence alignment using artificial neural networks:  
518 application to the MHC class I system. *Bioinformatics* .
- 519 5. Deres, K., T. N. Schumacher, K. H. Wiesmuller, S. Stevanovic, G. Greiner, G. Jung, and H. L. Ploegh.  
520 1992. Preferred size of peptides that bind to H-2 Kb is sequence dependent. *Eur J Immunol* 22: 1603–8.
- 521 6. Trolle, T., C. P. McMurtrey, J. Sidney, W. Bardet, S. C. Osborn, T. Kaever, A. Sette, W. H.  
522 Hildebrand, M. Nielsen, and B. Peters. 2016. The Length Distribution of Class I-Restricted T Cell  
523 Epitopes Is Determined by Both Peptide Supply and MHC Allele-Specific Binding Preference. *J Immunol*  
524 196: 1480–7.
- 525 7. Lundegaard, C., K. Lamberth, M. Harndahl, S. Buus, O. Lund, and M. Nielsen. 2008. NetMHC-3.0:  
526 accurate web accessible predictions of human, mouse and monkey MHC class I affinities for peptides of  
527 length 8-11. *Nucleic Acids Res* 36.
- 528 8. Nielsen, M., C. Lundegaard, T. Blicher, K. Lamberth, M. Harndahl, S. Justesen, G. Roder, B. Peters,  
529 A. Sette, O. Lund, and S. Buus. 2007. NetMHCpan, a method for quantitative predictions of peptide  
530 binding to any HLA-A and -B locus protein of known sequence. *PLoS ONE* 2: e796.
- 531 9. Kreiter, S., M. Vormehr, N. van de Roemer, M. Diken, M. Löwer, J. Diekmann, S. Boegel, B. Schrörs,  
532 F. Vascotto, J. C. Castle, A. D. Tadmor, S. P. Schoenberger, C. Huber, Ö. Türeci, and U. Sahin. 2015.  
533 Mutant MHC class II epitopes drive therapeutic immune responses to cancer. *Nature* 520: 692–696.
- 534 10. Gubin, M. M., M. N. Artyomov, E. R. Mardis, and R. D. Schreiber. 2015. Tumor neoantigens:  
535 building a framework for personalized cancer immunotherapy. *J. Clin. Invest.* 125: 3413–3421.
- 536 11. 2017. The problem with neoantigen prediction. *Nat. Biotechnol.* 35: 97.
- 537 12. Tenzer, S., B. Peters, S. Bulik, O. Schoor, C. Lemmel, M. M. Schatz, P. M. Kloetzel, H. G.  
538 Rammensee, H. Schild, and H. G. Holzhtuter. 2005. Modeling the MHC class I pathway by combining  
539 predictions of proteasomal cleavage, TAP transport and MHC class I binding. *Cell Mol Life Sci* 62: 1025–  
540 37.
- 541 13. Harndahl, M., M. Rasmussen, G. Roder, I. Dalgaard Pedersen, M. Sorensen, M. Nielsen, and S. Buus.  
542 2012. Peptide-MHC class I stability is a better predictor than peptide affinity of CTL immunogenicity.  
543 *Eur J Immunol* 42: 1405–16.
- 544 14. Bassani-Sternberg, M., C. Chong, P. Guillaume, M. Solleder, H. Pak, P. O. Gannon, L. E. Kandalaft,  
545 G. Coukos, and D. Gfeller. 2017. Deciphering HLA-I motifs across HLA peptidomes improves neo-  
546 antigen predictions and identifies allosteric regulating HLA specificity. *PLOS Comput. Biol.* 13:  
547 e1005725.
- 548 15. Abelin, J. G., D. B. Keskin, S. Sarkizova, C. R. Hartigan, W. Zhang, J. Sidney, J. Stevens, W. Lane,  
549 G. L. Zhang, T. M. Eisenhaure, K. R. Clauser, N. Hacohen, M. S. Rooney, S. A. Carr, and C. J. Wu.  
550 2017. Mass Spectrometry Profiling of HLA-Associated Peptidomes in Mono-allelic Cells Enables More  
551 Accurate Epitope Prediction. *Immunity* 46: 315–326.

- 552 16. Bassani-Sternberg, M., and D. Gfeller. 2016. Unsupervised HLA Peptidome Deconvolution Improves  
553 Ligand Prediction Accuracy and Predicts Cooperative Effects in Peptide-HLA Interactions. *J. Immunol.*  
554 *Baltim. Md 1950* 197: 2492–2499.
- 555 17. Pearson, H., T. Daouda, D. P. Granados, C. Durette, E. Bonneil, M. Courcelles, A. Rodenbrock, J.-P.  
556 Laverdure, C. Côté, S. Mader, S. Lemieux, P. Thibault, and C. Perreault. 2016. MHC class I-associated  
557 peptides derive from selective regions of the human genome. *J. Clin. Invest.* 126: 4690–4701.
- 558 18. Bassani-Sternberg, M., E. Bräunlein, R. Klar, T. Engleitner, P. Sinitcyn, S. Audehm, M. Straub, J.  
559 Weber, J. Slotta-Huspenina, K. Specht, M. E. Martignoni, A. Werner, R. Hein, D. H Busch, C. Peschel,  
560 R. Rad, J. Cox, M. Mann, and A. M. Krackhardt. 2016. Direct identification of clinically relevant  
561 neoepitopes presented on native human melanoma tissue by mass spectrometry. *Nat. Commun.* 7: 13404.
- 562 19. Sidney, J., S. Southwood, C. Oseroff, M. F. del Guercio, A. Sette, and H. M. Grey. 2001.  
563 Measurement of MHC/peptide interactions by gel filtration. *Curr. Protoc. Immunol.* Chapter 18: Unit  
564 18.3.
- 565 20. Harndahl, M., S. Justesen, K. Lamberth, G. Roder, M. Nielsen, and S. Buus. 2009. Peptide binding to  
566 HLA class I molecules: homogenous, high-throughput screening, and affinity assays. *J. Biomol. Screen.*  
567 14: 173–80.
- 568 21. Nielsen, M., C. Lundegaard, P. Worning, S. L. Lauemoller, K. Lamberth, S. Buus, S. Brunak, and O.  
569 Lund. 2003. Reliable prediction of T-cell epitopes using neural networks with novel sequence  
570 representations. *Protein Sci* 12: 1007–17.
- 571 22. Bassani-Sternberg, M., S. Pletscher-Frankild, L. J. Jensen, and M. Mann. 2015. Mass spectrometry of  
572 human leukocyte antigen class I peptidomes reveals strong effects of protein abundance and turnover on  
573 antigen presentation. *Mol Cell Proteomics* 14: 658–73.
- 574 23. Jorgensen, K. W., M. Rasmussen, S. Buus, and M. Nielsen. 2013. NetMHCstab - predicting stability  
575 of peptide:MHC-I complexes; impacts for CTL epitope discovery. *Immunology* .
- 576 24. Paul, S., D. Weiskopf, M. A. Angelo, J. Sidney, B. Peters, and A. Sette. 2013. HLA class I alleles are  
577 associated with peptide-binding repertoires of different size, affinity, and immunogenicity. *J Immunol*  
578 191: 5831–9.
- 579 25. Bjerregaard, A.-M., M. Nielsen, S. R. Hadrup, Z. Szallasi, and A. C. Eklund. 2017. MuPeXI:  
580 prediction of neo-epitopes from tumor sequencing data. *Cancer Immunol. Immunother. CII* .
- 581 26. Karosiene, E., M. Rasmussen, T. Blicher, O. Lund, S. Buus, and M. Nielsen. 2013. NetMHCIIpan-  
582 3.0, a common pan-specific MHC class II prediction method including all three human MHC class II  
583 isotypes, HLA-DR, HLA-DP and HLA-DQ. *Immunogenetics* 65: 711–24.
- 584 27. Murphy, J. P., P. Konda, D. J. Kowalewski, H. Schuster, D. Clements, Y. Kim, A. M. Cohen, T.  
585 Sharif, M. Nielsen, S. Stevanovic, P. W. Lee, and S. Gujar. 2017. MHC-I Ligand Discovery Using  
586 Targeted Database Searches of Mass Spectrometry Data: Implications for T-Cell Immunotherapies. *J.*  
587 *Proteome Res.* 16: 1806–1816.
- 588 28. Rasmussen, M., E. Fenoy, M. Harndahl, A. B. Kristensen, I. K. Nielsen, M. Nielsen, and S. Buus.  
589 2016. Pan-Specific Prediction of Peptide-MHC Class I Complex Stability, a Correlate of T Cell  
590 Immunogenicity. *J Immunol* 197: 1517–24.
- 591 29. Andreatta, M., B. Alvarez, and M. Nielsen. 2017. GibbsCluster: unsupervised clustering and  
592 alignment of peptide sequences. *Nucleic Acids Res.* .
- 593 30. Thomsen, M. C., and M. Nielsen. 2012. Seq2Logo: a method for construction and visualization of  
594 amino acid binding motifs and sequence profiles including sequence weighting, pseudo counts and two-  
595 sided representation of amino acid enrichment and depletion. *Nucleic Acids Res* 40: W281-7.
- 596 31. Bassani-Sternberg, M., C. Chong, P. Guillaume, M. Solleder, H. Pak, P. O. Gannon, L. E. Kandalaft,  
597 G. Coukos, and D. Gfeller. 2017. Deciphering HLA-I motifs across HLA peptidomes improves neo-  
598 antigen predictions and identifies allosteric regulating HLA specificity. *bioRxiv* 98780.

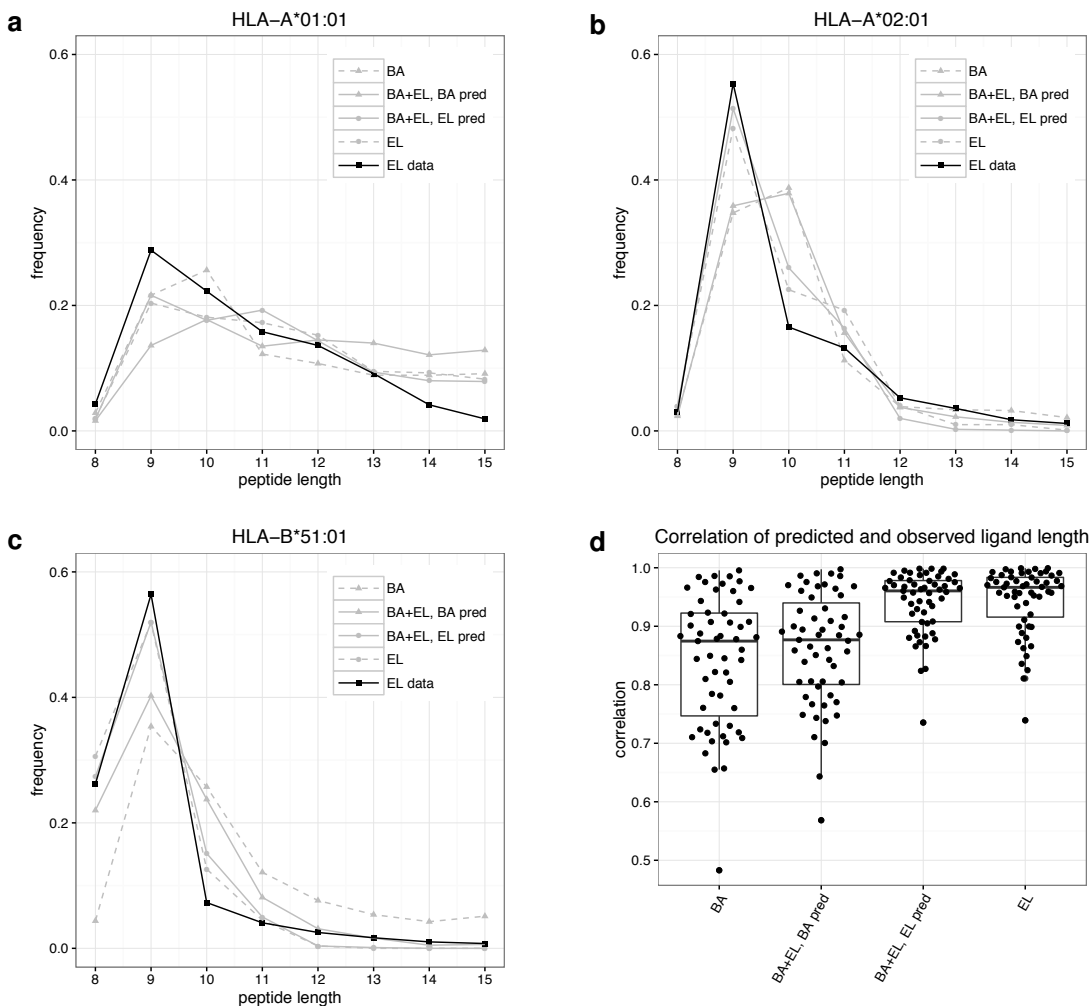
601 **Figures**



602 **Figure 1:** Visualization of the neural networks with two output neurons used for combined  
603 training on binding affinity and eluted ligand data.  
604  
605

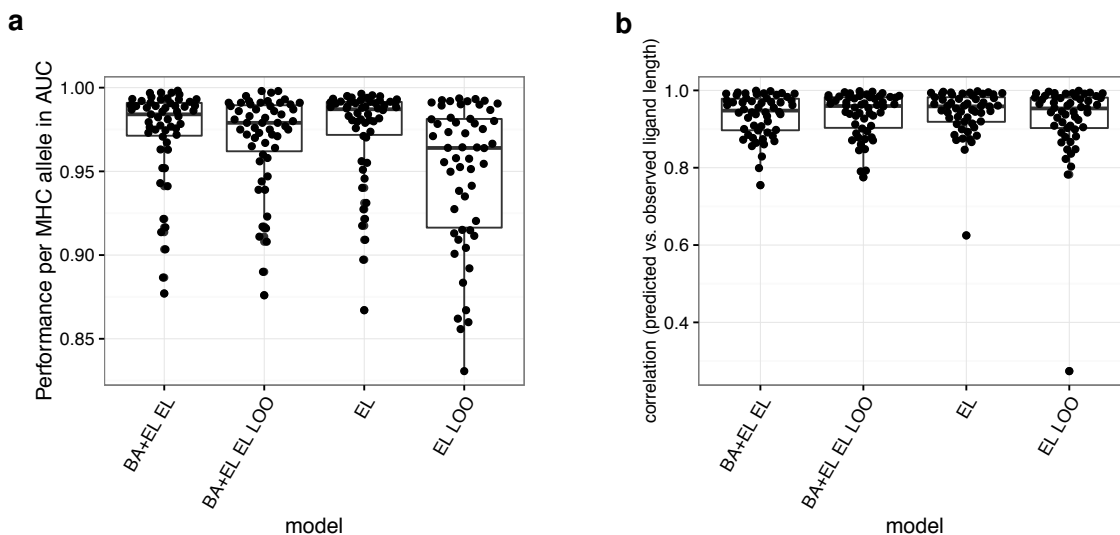


606 **Figure 2:** Mean performance per MHC molecule measured in terms of AUC for the four  
607 methods; BA (trained on binding affinity data only), EL (trained on eluted ligand data only),  
608 BA+EL BA (the binding affinity prediction value of the model trained on the combined binding  
609 affinity and eluted ligand data), and BA+EL EL (the eluted ligand likelihood prediction value of  
610 the model trained on the combined binding affinity and eluted ligand data) The methods were  
611 evaluated on all binding affinity (all\_BA) data and all eluted ligand (all\_EL) data including  
612 negative peptides derived from source proteins, and on data sets restricted to alleles occurring in  
613 both binding affinity and eluted ligand data sets (shared\_BA, and shared\_EL).  
614  
615

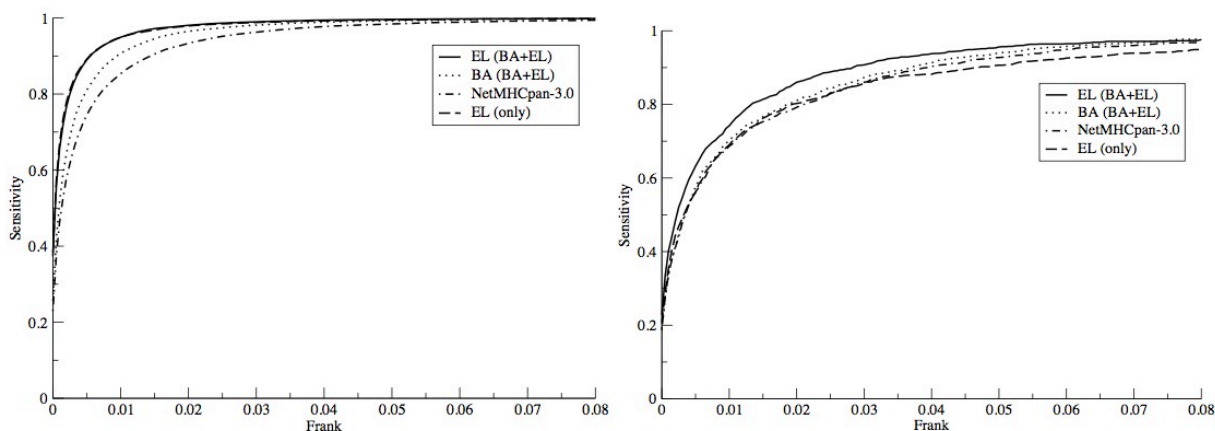


616  
 617 **Figure 3: a-c)** Predicted length preference of selected MHC molecules according to different  
 618 models. Binding to selected HLA molecules was predicted for 80,000 8-15-mer peptides and the  
 619 frequency of peptide lengths in the top 2% predicted peptides calculated. **d)** Correlation of  
 620 predicted and observed ligand length for different models. Binding to all HLA alleles present in  
 621 both binding affinity and eluted ligand data sets was predicted using the four different prediction  
 622 methods for 80,000 8-15-mer peptides. Subsequently, the occurrence of different peptide lengths  
 623 in the top 2% predicted peptides for each molecule was calculated, and the correlation coefficient  
 624 between these frequencies and the length frequencies in the eluted ligand data set calculated.  
 625

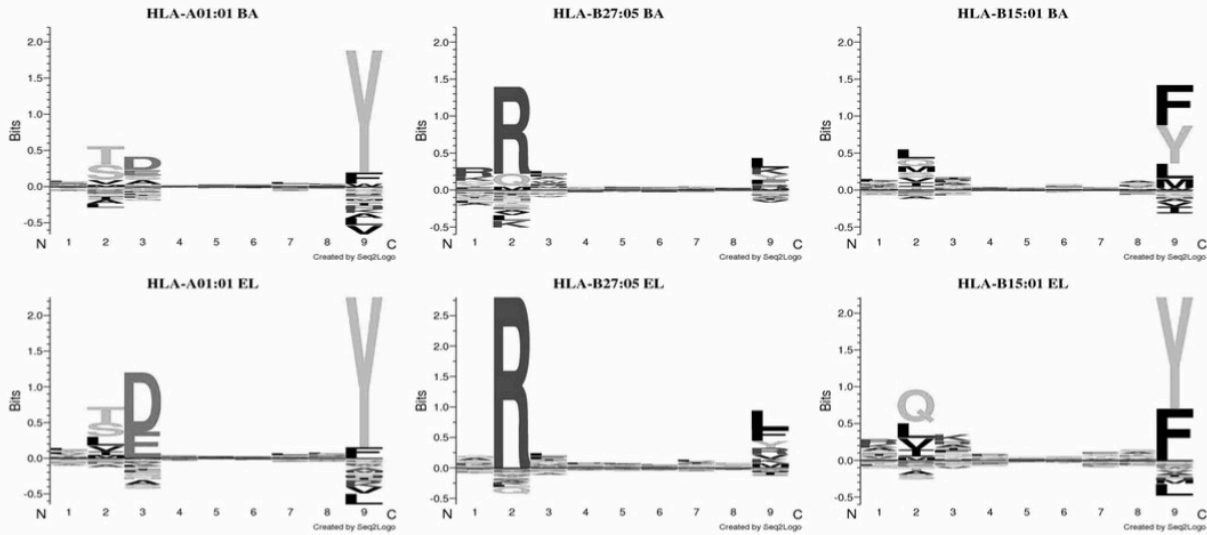




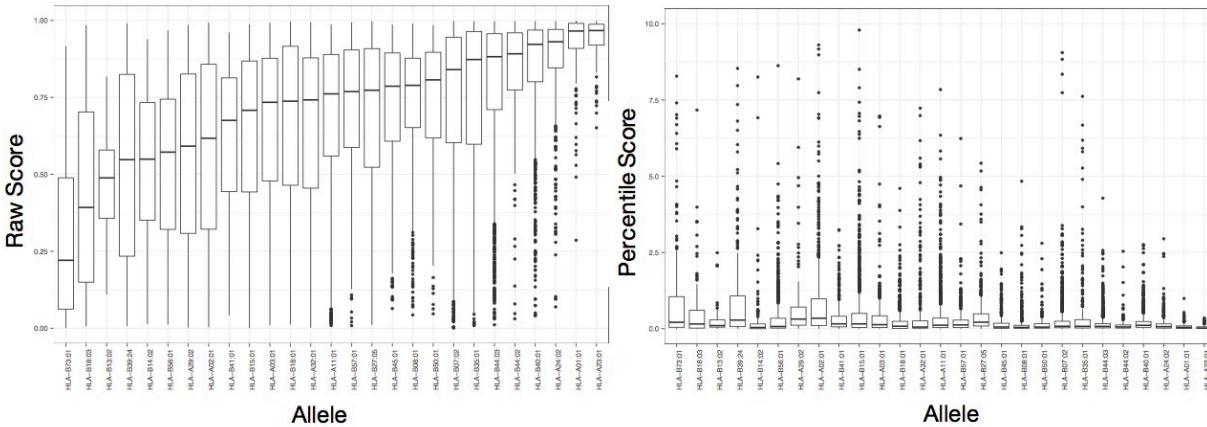
626  
627 **Figure 4:** Eluted ligand leave-one-out experiments. **a)** Performance per MHC allele of a model  
628 trained on all data and a model where the eluted ligand data of a given allele was left out of the  
629 training process. **b)** Correlation of predicted and observed ligand length for a model trained on  
630 all data and the leave-one-out models.  
631



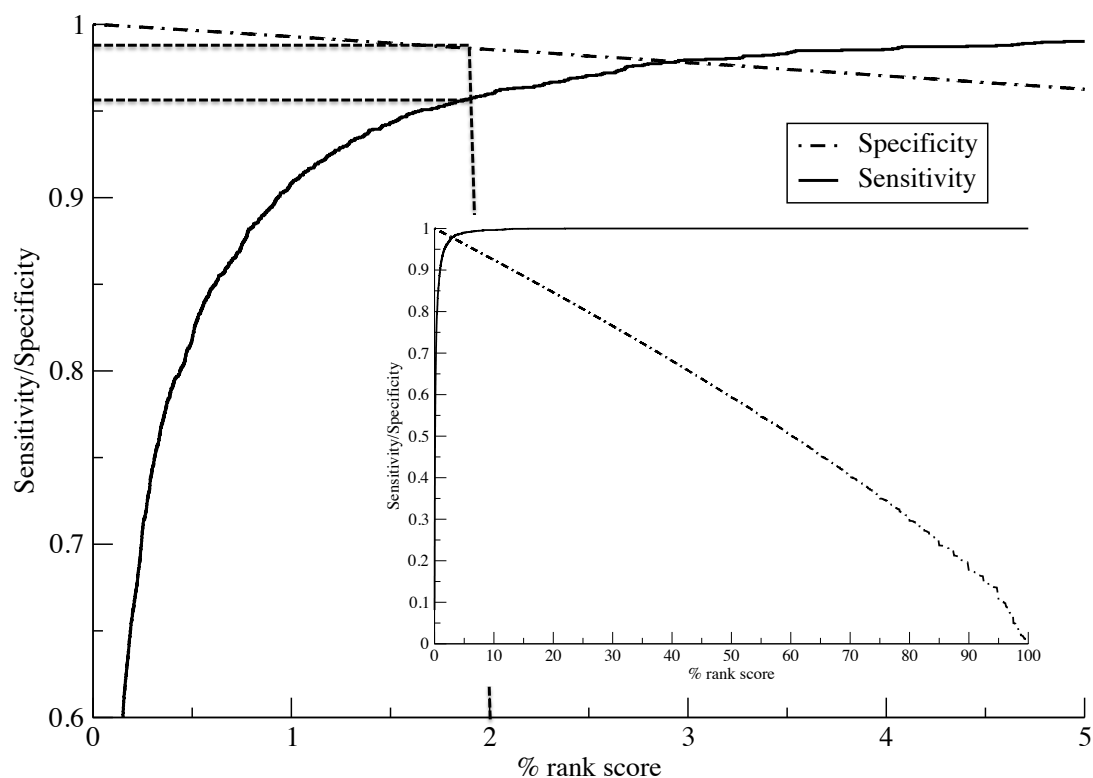
632  
633 **Figure 5:** Sensitivity of different models as a function of the Frank threshold on **a)** eluted ligands  
634 published by Pearson et al. (17) and **b)** T-cell epitope data downloaded from IEDB.  
635



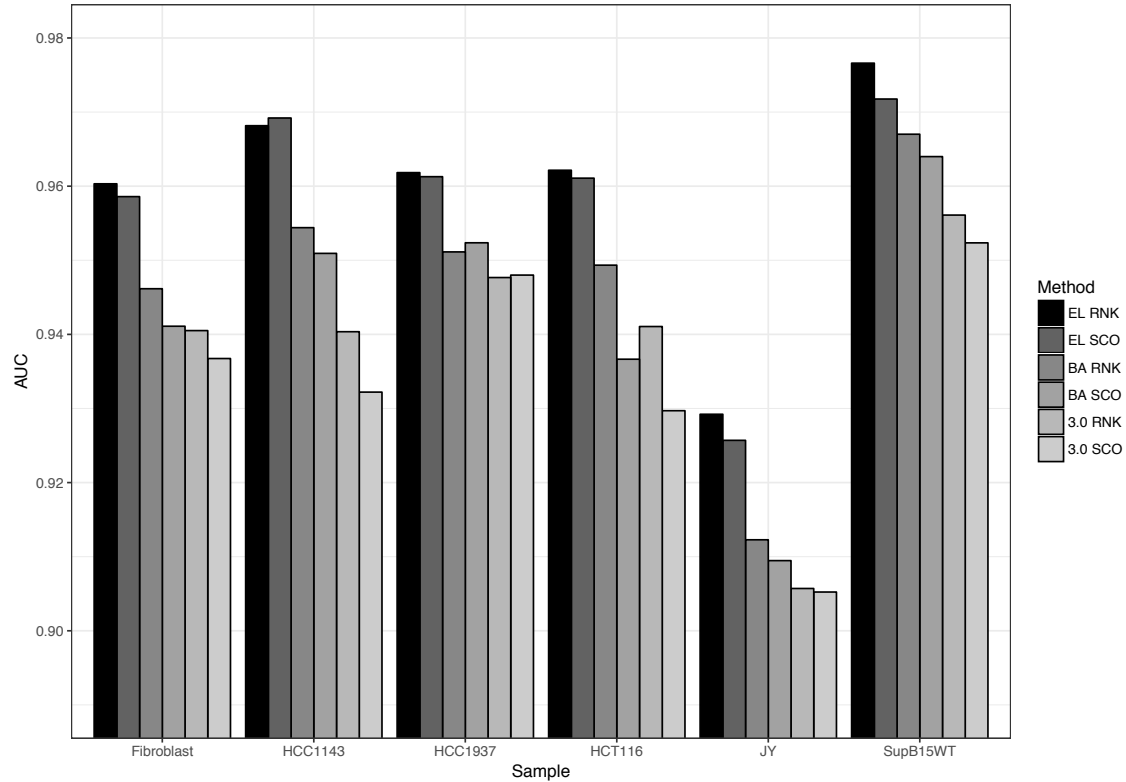
636  
 637 **Figure 6:** Binding motifs for HLA molecules derived from (upper panel) in-vitro binding  
 638 affinity data using a binding threshold of 500 nM, (lower panel) eluted ligand data. Logos were  
 639 made using Seq2Logo with default parameters (30).  
 640



641  
 642 **Figure 7:** Motivation for using percentile rank score predictions. Box-plot representation of  
 643 prediction values for the ligands in the Pearson data set. Left panel: Eluted ligand likelihood  
 644 prediction scores. Right panel: Percentile rank values.  
 645



646  
 647 **Figure 8:** Sensitivity and specificity performance curves for the NetMHCpan-4.0 eluted ligand  
 648 likelihood predictions. Curves are estimated from a balanced set of eluted ligands from the (17)  
 649 data set. The insert shows the complete sensitivity and specificity curves as a function of the  
 650 percentile rank score. The main plot shows the curves in the high-scoring range for 0-5 percentile  
 651 scores. Dotted vertical and horizontal lines are guides to the eye indicating sensitivity and  
 652 specificity and the 2% rank score threshold.  
 653



654 **Figure 9:** Predictive performance measured in terms of AUC on the Bassani-Sternberg unfiltered  
 655 eluted ligand data sets. Prediction values are assigned to each peptide in a given data set as the  
 656 lowest percentile rank score / highest prediction score to each of the HLA molecule expressed by  
 657 the given cell line. The six methods included are: EL RNK (NetMHCpan-4.0 eluted ligand  
 658 percentile rank), EL SCO (NetMHCpan-4.0 eluted ligand likelihood score), BA RNK  
 659 (NetMHCpan-4.0 binding affinity percentile rank), BA SCO (NetMHCpan-4.0 binding affinity  
 660 score), 3.0 RNK (NetMHCpan-3.0 percentile rank, and 3.0 SCO (NetMHCpan-3.0 binding  
 661 affinity score).

662  
 663  
 664  
 665

Sample	Ligand	NetMHCpan-4.0	NetMHCpan-3.0	Bassani-Sternberg et al.	#peptides
Mel8	SPGPVKLEL	<b>1 (0.0124)</b>	12	2	1340
Mel5	YIDERFERY	15 (0.0077)	33	<b>3</b>	25807
Mel5	ETSKQVTRW	189 (0.1156)	464	<b>13</b>	25807
Mel15	GRIAFFLKY	21 (0.0098)	224	<b>3</b>	24766
Mel15	LPIQYEPVL	10 (0.0071)	24	7	24766
Mel15	KLKLPIMK	<b>6 (0.0061)</b>	34	21	24766
Mel15	GRTGAGKSFL	1226 (0.6909)	2186	<b>243</b>	24766
Mel15	KLILWRGLK	457 (0.2364)	<b>112</b>	527	24766
Mel15	ASWVVPIDIK	1629 (0.9723)	<b>1278</b>	3978	24766
12T	DANSFLQSV	<b>19 (0.0205)</b>	944	38	15750

666  
667 **Figure 10:** Predictive performance evaluated in terms of rank of neo-antigens identified in four  
668 melanoma samples. A rank value of 1 corresponds to the ligand obtaining the highest score  
669 (lowest percentile rank) of all peptides from the given sample. Data and performance values for  
670 MixMHCpred are from (31). NetMHCpan-4.0 and NetMHCpan-3.0 are performance values  
671 obtained by assigning to each peptide in the given data set the lowest percentile rank score to  
672 each of the HLA-A and B molecules expressed by the given cell line. The values in parentheses  
673 for NetMHCpan-4.0 are the predicted percentile rank values. Lowest rank value for each ligand  
674 is highlighted in bold.  
675